THE JOURNAL OF BIOLOGICAL CHEMISTRY VOL. 291, NO. 19, pp. 9906–9919, May 6, 2016
Published in the U.S.A.

Drosophila *O*-GlcNAcase Deletion Globally Perturbs Chromatin *O*-GlcNAcylation*[S]

Received for publication, November 18, 2015, and in revised form, March 7, 2016 Published, JBC Papers in Press, March 8, 2016, DOI 10.1074/jbc.M115.704783

Ilhan Akan[‡], Dona C. Love[§], Katryn R. Harwood[‡], Michelle R. Bond[‡], and John A. Hanover[‡1]
From the [‡]NIDDK and [§]NCI,National Institutes of Health, Bethesda, Maryland 20892

Gene expression during *Drosophila* development is subject to regulation by the Polycomb (Pc), Trithorax (Trx), and Compass chromatin modifier complexes. *O*-GlcNAc transferase (OGT/SXC) is essential for Pc repression suggesting that the *O*-GlcNAcylation of proteins plays a key role in regulating development. OGT transfers *O*-GlcNAc onto serine and threonine residues in intrinsically disordered domains of key transcriptional regulators; *O*-GlcNAcase (OGA) removes the modification. To pinpoint genomic regions that are regulated by *O*-GlcNAc levels, we performed ChIP-chip and microarray analysis after OGT or OGA RNAi knockdown in S2 cells. After OGA RNAi, we observed a genome-wide increase in the intensity of most *O*-GlcNAc-occupied regions including genes linked to cell cycle, ubiquitin, and steroid response. In contrast, *O*-GlcNAc levels were strikingly insensitive to OGA RNAi at sites of polycomb repression such as the Hox and NK homeobox gene clusters. Microarray analysis suggested that altered *O*-GlcNAc cycling perturbed the expression of genes associated with morphogenesis and cell cycle regulation. We then produced a viable null allele of *oga* (*oga*$^{del.1}$) in *Drosophila* allowing visualization of altered *O*-GlcNAc cycling on polytene chromosomes. We found that trithorax (TRX), absent small or homeotic discs 1 (ASH1), and Compass member SET1 histone methyltransferases were *O*-GlcNAc-modified in *oga*$^{del.1}$ mutants. The *oga*$^{del.1}$ mutants displayed altered expression of a distinct set of cell cycle-related genes. Our results show that the loss of OGA in *Drosophila* globally impacts the epigenetic machinery allowing *O*-GlcNAc accumulation on RNA polymerase II and numerous chromatin factors including TRX, ASH1, and SET1.

Epigenetic regulation of gene expression during development is essential for proper cell fate determination. Epigenetic modifiers act by modifying chromatin and thereby altering chromatin structure. The Polycomb (Pc)[2] repressor and Trithorax (Trx) and Compass activator complexes play major roles in maintaining gene expression profiles required for proper body plan formation. Methylation of several lysine residues of histone 3 are among the best understood epigenetic modifications. The trimethylation of histone 3 lysine 27 (H3K27me3) by Polycomb repressive complex 2 (PRC2) member Enhancer of zeste (E(z)) is a repressive transcription mark (1–3). In contrast, histone 3 lysine 4 monomethylation (H3K4me) performed by TRX, histone 3 lysine 36 dimethylation (H3K36me2) by ASH1, and histone 3 lysine 4 trimethylation (H3K4me3) by Compass member SET1 are activating modifications in *Drosophila* (4, 5). Pc group member super sex combs (*ogt*/*sxc*) encodes the *Drosophila* *O*-GlcNAc transferase (OGT), which regulates Pc-mediated repression by post translationally *O*-GlcNAcylating and stabilizing Polyhomeotic (Ph), a member of PRC1 in *Drosophila* (6–8). Ph forms large protein aggregates and cannot function in *ogt* mutants, leading to homeotic defects (7, 9). Moreover, it has been shown that knockdown of mammalian OGT decreases H3K27me3 levels by affecting the stability of E(z) homolog 2 (EZH2) in the MCF7 breast cancer cell line (1).

The hexosamine biosynthetic pathway generates UDP-GlcNAc using glucose, glutamine, acetyl-CoA, and UTP. Therefore changes in the intracellular levels of these nutrition-derived products directly influence the cellular concentration of UDP-GlcNAc making it sensitive to nutrient levels. OGT then catalyzes the addition of *O*-GlcNAc onto hydroxyl groups of serine/threonine residues of proteins using the nutrient sensor UDP-GlcNAc as a substrate. The *O*-GlcNAc modification on nucleocytoplasmic proteins is then removed by the enzyme *O*-GlcNAcase (OGA) in a dynamic fashion, modulating intracellular events ranging from transcription to cell cycle regulation (10, 11). *O*-GlcNAcylation, like phosphorylation, can impact protein function, localization, and/or expression levels (12, 13). The singularity of the OGT and OGA enzymes, the rapidity with which *O*-GlcNAc cycles, and the diversity of protein substrates poises this post-translational modification to play a critical role in modulating the rapid cellular changes required for proper development (14–17).

O-GlcNAc was first detected on *Drosophila* polytene chromosomes (18) and later found at the promoter regions of *Caenorhabditis elegans* genes that are involved in a wide variety of pathways ranging from metabolism to aging (19). In addition to its role in Pc repression, OGT is thought to have additional roles in epigenetic regulation in mammals. First, OGT can directly *O*-GlcNAcylate chromatin remodelers like Sin3A and SET1DA (14, 17). Although controversial, OGT is argued to directly *O*-GlcNAc modify histone 2B, thereby altering chromatin structure (20, 21). Beyond affecting gene expression

* This work was supported, in whole or in part, by an NIDDK, National Institutes of Health Intramural Grant. The content is solely the responsibility of the authors and does not necessarily represent the official views of the National Institutes of Health. The authors declare that they have no conflicts of interest with the contents of this article
[S] This article contains supplemental Figs. S1 and S2.
[1] To whom correspondence should be addressed: LCBB, NIDDK, National Institutes of Health, 8 Center Dr., Bethesda, MD 20892. Tel.: 301-496-0943; Fax: 301-946-9431; E-mail: jah@helix.nih.gov.
[2] The abbreviations used are: Pc, polycomb; Trx, Trithorax; PRC2, polycomb repressive complex 2; ASH1, absent small or homeotic discs 1; OGT, *O*-GlcNAc transferase; Ph, polyhomeotic; OGA, *O*-GlcNAcase; RNA Pol II, RNA polymerase II; FdGlcNAc, fluorescein di(*N*-acetyl-β-D-glucosaminide); IP, immunoprecipitate; HCF, host cell factor.

through directly or indirectly changing chromatin, *O*-GlcNAc influences transcription by affecting the activity and/or stability of key players including RNA polymerase II (RNA Pol II) and many transcription factors (11, 16, 22–26). Furthermore, *O*-GlcNAc is known to play a role in cell cycle progression with the transcriptional co-regulator host cell factor 1 (HCF1) having been identified as an OGT target (27). Indeed, HCF1 needs to be *O*-GlcNAcylated and cleaved by OGT to regulate cell division (27). *O*-GlcNAcylation plays a key role in mitosis as overexpression of OGT or inhibition of OGA impairs cell cycle progression (28). Last, the *O*-GlcNAc modification of histones in a cell cycle-dependent manner may prime this post-translational modification to influence cell cycle and gene expression (29, 30).

To better understand how *O*-GlcNAc cycling influences gene expression and which genomic regions are more susceptible to changing *O*-GlcNAc levels, we altered *O*-GlcNAc levels by knocking down either OGT or OGA expression by RNAi and performed ChIP-chip for *O*-GlcNAc and other chromatin associated factors followed by gene expression analysis in *Drosophila* Schneider 2 (S2) cells. An indicator of active transcription, phosphorylated serine 2 on the carboxyl-terminal tail of RNA polymerase II (RNA Pol II Ser2P) was generally at low levels at sites of *O*-GlcNAc modified chromatin including the Pho-enriched Hox gene clusters suggesting that the *O*-GlcNAc modification is mainly associated with transcriptionally silent regions. Interestingly, *O*-GlcNAc occupies additional sites on chromatin other than Pho co-occupied sites. A number of these Pho independent *O*-GlcNAc occupied chromatin regions were shared with RNA Pol II Ser2P underscoring that *O*-GlcNAc plays a role in active transcription as well. Gene expression profiling of these cells revealed that *O*-GlcNAc levels most significantly affect pathways including cell cycle and metabolism. Intrigued by the presence of *O*-GlcNAc on transcriptionally silent and active chromatin regions, we elected to study the consequences of a permanent increase in *O*-GlcNAc levels in the whole animal by generating a null allele of *oga* in *Drosophila* ($oga^{del.1}$). In $oga^{del.1}$ mutant animals *O*-GlcNAc cycling on chromatin was globally perturbed when visualized on polytene chromosomes. We determined that Trithorax members TRX and ASH1, and Compass member SET1 histone methyltransferases are *O*-GlcNAc modified in $oga^{del.1}$ mutants. Furthermore, expression of specific cell cycle-related genes, including host cell factor, were altered in *oga* mutant ovaries. Our findings directly demonstrate that *O*-GlcNAc cycling is an important part of the epigenetic machinery in *Drosophila*.

Experimental Procedures

Drosophila S2 Cell Culture and RNAi Treatment—S2 cells were cultured in Schneider's *Drosophila* medium supplemented with 10% FBS.

RNAi knockdown of OGT and OGA in S2 cells was performed as described previously (31). Briefly, genomic DNA was isolated from S2 cells with DNAeasy kit (Qiagen). OGT, OGA, or GFP specific primers were designed to include a T7 RNA polymerase binding site. The PCR product is then *in vitro* transcribed to generate dsRNA (T7 MEGAscript Kit, Ambion). dsRNA was purified with the RNAeasy kit (Qiagen) and transfected to S2 cells. Cells were harvested to isolate RNA for transcriptomics or chromatin isolation for ChIP-chip analysis 3 days after transfection.

Antibodies Used for ChIP-chip—Mouse anti-*O*-GlcNAc (Thermo Scientific, MA1-076) and rabbit anti-RNA Pol II Ser2P (Abcam, ab5095) antibodies were used. Pho antibody was described earlier (32). After chromatin purification, Pho, *O*-GlcNAc, and RNA Pol II Ser2P ChIP-chip was performed by a minor modification of the method described previously (19).

Whole Genome Transcriptome Analysis—Transcriptome analysis was performed using Affymetrix Genechip *Drosophila* Genome 1.0 Arrays. cDNA was prepared using Smartscribe prior to library synthesis according to the manufacturer's instructions. Statistical analysis was performed as previously described (19).

ChIP-on-Chip Analysis—ChIP-chip analysis was carried out in *Drosophila* S2 cells by a modification of the method described previously using anti-*O*-GlcNAc antibody (mouse HGAC-85) (19).

Probe Signal and Enrichment Analysis—Analysis was performed using Affymetrix GeneChip *Drosophila* Tiling 1.0R Arrays and analyzed using Affymetrix build 5 (for NCBI). The CEL files (Cell Intensity Files; containing processed image data of the array scans) were analyzed using Affymetrix Tiling Analysis Software (TAS version 1.1.02). A two-sample analysis was performed comparing each CEL file of the ChIP/IP samples against the CEL file from the input DNA array. This analysis generates BAR (binary analysis results) files that contain the signal values for all probes on the arrays. Signal values are "estimates of-fold enrichment" of ChIP/IP-DNA, which in essence are ratios (in linear scale) between the intensity of the probes on the ChIP/IP array divided by the intensity of the corresponding probe on the input DNA array. To make the values more significant, however, these ratios are computed by applying averaging and ranking steps to a set of probes within a 400 – 800-bp sliding window. The TAS parameters used for binary analysis results file generation are given in the summary file (sheet: TAS parameters; "Analyze Intensities").

Interval Analysis—An interval is a discrete genomic region, defined by the chromosome number and a start and end coordinate. Intervals represent the locations of signal peaks. For each binary analysis results file, intervals are calculated using Affymetrix TAS and compiled into BED files (browser extensible data). Ratios of normalized averaged signal intensities between Chips were used to calculate fold-enrichment between OGA, WT control (GFP), and OGT knockdown experiments. The co-enrichment of *O*-GlcNAc, Pho, RNA Pol II Ser2P, and other chromatin factors were determined using Affymetrix Tiling Analysis Software version 1.1.

Two-sample Analysis—In this analysis pipeline, for each tiling probe, an enrichment is estimated, and this involves combining two statistical approaches: the Wilcoxon signed-ran test (a nonparametric paired difference test) and the Hodges-Lehmann estimator (a robust and nonparametric estimator of the location parameter of a population). All of the peaks we reported had significant co-enrichments as determined by the statistical tests mentioned above; these are the values used to populate the co-enrichment table. The ChIP-chip and gene

expression microarray experiments were both done in triplicate. Data were submitted in the GEO database as GSE74846.

Functional Annotation Clustering—Functional annotation clustering is a tool in version 6.7 of DAVID available (david.abcc.ncifcrf.gov) for annotation, visualization, and integrated discovery that analyzes enrichment in related gene sets into clusters by using a variety of assembled gene sets in biological pathways. For ChIP-chip analysis, we identified the group of genes that had *O*-GlcNAc occupied regions that showed little or no increase (0.5–1), moderately increased (1–1.5), and highly increased (1.5–2.25) with respect to *O*-GlcNAc levels following OGA RNAi using high classification stringency. For each clustering analysis only the most highly enriched two groups was shown. The same functional clustering with medium stringency was used to analyze genes whose expression was altered by changes in *O*-GlcNAc cycling. Genes that showed 1.5-fold or more change in expression were used for OGT RNAi, and genes that displayed altered expression of 1.2-fold were used for OGA RNAi.

Fly Stocks—13618 OGA P element insertion, *ogt*/*sxc* mutants, Tubulin Gal4, Actin-Gal4, Nanos Gal4, transposase lines, and the two deficiency lines spanning the *oga* gene, B9485 and B9487, were from the Bloomington Stock Center. The UAS-OGA-RNAi fly line was obtained from VDRC (33). The reported UAS-OGA overexpression lines were originally generated by Kaasik *et al.* (34). $oga^{del.1}$ mutant was generated by standard P-element excision protocol (35). $oga^{del.1}$ mosaics were generated using the FRT/FLP recombination system (36). Flies were maintained at 25 °C in a humidified incubator. *Drosophila* MM media was purchased from KD Medical (Columbia, MD).

Polytene Chromosome Staining and Imaging—Polytene chromosomes were prepared as described previously (37). For staining, the slides containing polytenes were incubated with 100, 50, and 25% ethanol followed by PBS/Triton X-100 (0.1% Triton X-100). After 3 washes with PBS/Triton X-100, the slides were blocked with Odyssey blocking reagent for 1 h at room temperature, and incubated with ASH1, TRX, or SET1 at 1/50 dilution along with *O*-GlcNAc specific antibody at 1/100 dilution overnight at 4 °C in a humidified chamber. On the next day slides were washed 4 times with PBS/ Triton X-100 and incubated with Alexa Fluor-conjugated secondary antibodies in the dark for 2 h at room temperature. The slides were then mounted in Slowfade mounting medium (Invitrogen) and visualized using a Zeiss LSM 700 confocal microscope with Zen imaging software (Zeiss). Primary antibodies and dilutions used for staining were: rabbit anti-ASH1 (Novus number 50100002), anti-RNA Pol II Ser2P (Abcam, ab5095), anti-Polycomb (Santa Cruz, number sc-25762), and mouse HGAC-85 anti-*O*-GlcNAc (Thermo Scientific, number MA1-076). Rabbit anti-SET1 and anti-TRX antibodies were a kind gift from Dr. Shilatifard (38). All secondary antibodies were Alexa Fluor 488- or Alexa Fluor 568-conjugated (Invitrogen) and used at 1/250 dilution.

Immunoprecipitation—Flies were fed with fresh yeast paste for 3 days and ovaries were dissected in ice-cold PBS. Ovary extracts were prepared in T-PER tissue extraction buffer (Thermo) containing protease inhibitors (Roche Applied Science) in an Eppendorf tube with a hand held pellet pestle (Kontes). Samples were then homogenized further on a rocker for 1 h at 4 °C. After centrifugation for 5 min at 14,000 rpm at 4 °C, the supernatant was used for immunoprecipitation. 300 μg of protein was used for immunoprecipitation in 500 μl of PBS, Triton X-100. ASH1 (Novus, number 50100002), BRE1 (Novus, number 40280002), SET1, and TRX antibodies were described (38). All primary antibodies were used at 1/100 dilution. Samples with antibodies were kept on a rocker overnight at 4 °C. 25 μl of Protein A/G beads were added the next morning and samples were rocked another 2 h. Samples were then centrifuged at 1,000 rpm ($\sim 300 \times g$) for 5 min at 4 °C and washed three times with PBS/Triton X-100 for 15 min each. Immunoprecipitated proteins were loaded onto SDS-PAGE gel and Western blot was performed for the presence of *O*-GlcNAc.

Western Blotting—Ovary proteins extracts for Western blot analysis were prepared as described above with minor modifications. T-PER buffer was supplemented with 1% SDS and lysates were heated to 80 °C for 15 min followed by centrifugation at 4 °C for 10 min at 14,000 rpm. Supernatants were used for Western analysis. Rabbit anti-histone 3 and rabbit anti-H3K4me3 (Millipore, number 07-473) were used at 1/2000, rabbit anti-H3K9Ac (Abcam, number ab4441) was used at 1/500, mouse anti-actin (Abcam, number ab8224) was used at 1/3000. The following antibodies were used at 1/1000 dilution: rabbit anti-H3K27ac (Abcam, number ab4729), rabbit anti-H3K27me3 (Millipore, number 07-449), rabbit anti-H3K36me, rabbit anti-H3K36me2, rabbit anti-H3K36me3, mouse anti-*O*-GlcNAc (Thermo Scientific, number MA1-072). Briefly, membranes were blocked with Odyssey blocking buffer (Odyssey, number 927-40000) for 1 h, washed 3 times with PBST (0.1% Tween 20), incubated with primary antibodies overnight at 4 °C, then washed with PBST again. Secondary antibodies were Odyssey IR dye-conjugated used at 1/10,000 dilution for 1 h in the dark at room temperature. Membranes were imaged and band intensities were analyzed with Odyssey imaging equipment.

O-GlcNAcase Activity Assay—OGA assay was performed as described (39). Briefly, ovary protein lysates were prepared in T-PER buffer. 100 μg of WT or $oga^{del.1}$ lysate were added to a mixture of 200 μM fluorescein di(*N*-acetyl-β-D-glucosaminide) (FDGlcNAc) and 50 mM *N*-acetylgalactosamine (GalNAc), in 50 mM citrate/phosphate buffer, pH 6.5. To control for any background fluorescence of the FDGlcNAc substrate itself, T-PER was added to a mixture of FDGlcNAc and GalNAc in the citrate/phosphate buffer ("no lysate"). All reactions were incubated in the dark at 37 °C, with shaking at 100 rpm for 30 min. The reactions were quenched by adding Na_2CO_3 to a final concentration of 400 mM. Fluorescence was measured in 1-s intervals at the excitation wavelength of 485 nm and emission wavelength of 535 nm on a Wallac 1420 fluorometer (PerkinElmer Life Sciences). All assays were performed in triplicate. Student's *t* test was used for data analysis. The signal detected in the no lysate reactions was averaged, and this value was subtracted from each lysate measurement. Data are presented as the mean ± S.E.

RNA Extraction and RT-PCR Analysis—5-Day-old well fed females were used for this experiment. 15 female ovaries were dissected on ice-cold PBS and RNA was extracted using TRIzol

(Life Technologies, Inc.) according to the manufacturer's instructions. cDNA was prepared with Q-Script cDNA master mixture (Quanta). RT-PCR analysis was performed using a Applied Biosystems instrument. Student's *t* test on selected pairs was used to compare gene expression levels.

The following primers were used: bazooka: CGGCCGGCAAGGTAAGATAA, and GCTCGGTGCTTGCATTTCAT; Hcf, GACCAGTGGTGGGATGACTG and GGCACTGTCGATCCCTGAAT; Capicua, CCAGTGCGGCAGATGTTTTT and CAGTTTCTCCACTCGACTCACA; Bam, GACCAGCAGTTGGACCACAAT and CTCTAAGCAATCGCCGTGCAG; HTS, CTGGCCGAGGTGAAAACGTA and GCTACTCCTACGGATCACGC; SXL, TCCACTCGTGACAAGTCCAAC and CCCACCACTCGCCATCTTAAA; Pka-C1, CATCAGCCATTTCCCTCCGT and CGCTTTGCACTTGCTTCTGT; Embargoed, TTGGTTCCATATCCGGTGCTT and CGTGGATACTGTCCCACCAC; and Rpl32, CGCCACCAGTCGGATCGATATGCTAAGCTGTC and CGCGCTCGACAATCTCCTTGCGCTTCTT.

Fecundity Assay—6 Newly hatched male and females were placed in embryo collection chambers (Genesee Sci) with apple juice agar plates and fresh yeast paste. Flies were acclimated to the chamber in constant darkness for 2 days and changing the apple juice agar plate every 24 h. The number of eggs on the plates was counted daily for the following 3 days. Experiments were done in triplicate and repeated 3 times. Statistical analysis was done by Student's *t* test on selected pairs. Data are presented as the mean ± S.E.

Results

Interfering with O-GlcNAc Cycling Alters Chromatin-associated O-GlcNAc Levels and Gene Expression in S2 Cells—The Pc group consists of a set of proteins required for regulating proper body plan development by repressing the expression of Hox genes through compacting chromatin and making DNA inaccessible to RNA polymerase (40, 41). OGT plays a role in Pc repression in *Drosophila* (6) and is essential for the function of Pc by *O*-GlcNAcylating Ph (7). Moreover, OGT is a member of the Pc group in *Drosophila* (6, 8) and *ogt* mutant flies die as pharate adults displaying homeotic transformations (9). The undiscovered genomic regions responsible for the homeotic transformations observed in *ogt* mutant flies encouraged us to increase our understanding of the genome-wide relationship between *O*-GlcNAc and Pc repression in *Drosophila*. For this purpose, we analyzed *O*-GlcNAc, Pho, and active transcription indicator RNA Pol II Ser2P distribution on chromatin using ChIP-chip tiling arrays in S2 cells that have decreased or increased *O*-GlcNAc levels (following OGT or OGA RNAi, respectively). We reasoned that altered *O*-GlcNAc levels would change the distribution of repressed chromatin (to be observed by Pho distribution) and/or actively transcribed (to be observed by RNA Pol II Ser2P distribution) chromatin regions. ChIP-chip was used because we found that it better reflects quantitative differences in occupancy than ChIP-Seq. The data we have reported here are available in the GEO database as GSE74846. Analysis of these data suggested that *O*-GlcNAc and Pho co-occupied many chromatin regions including the Hox gene clusters, whereas RNA Pol II Ser2P was excluded from those same regions (Fig. 1*a*). After OGA RNAi, *O*-GlcNAc levels were increased more than 2-fold (Fig. 1*b*). The number and amplitude of *O*-GlcNAc peaks on chromatin were also significantly increased (Fig. 1*c*, *red lines*) compared with the control sample (Fig. 1*c*, *blue line*).

Importantly, all ~8000 observable *O*-GlcNAc peaks were dramatically decreased by OGT RNAi (Fig. 1*c*, *green line*). The *O*-GlcNAc peak intervals associated with most genes showed a substantial increase (1.4-fold average) upon silencing of OGA. Based on the involvement of OGT in Pc repression and the homeotic transformations seen in *ogt* mutants, we expected to see altered *O*-GlcNAc occupancy on areas surrounding Hox genes upon disruption of *O*-GlcNAc cycling by loss of OGA. To our surprise, DAVID clustering analysis showed that the homeotic genes were 23-fold enriched in the small fraction of genes showing little if any change in *O*-GlcNAc levels after loss of OGA (OGA/WT ratio of 0.5–1.0-fold) (Fig. 1*d*) (42). Interestingly, DAVID clustering (42) also revealed that cell cycle-related genes were among those enriched for increased *O*-GlcNAc peak intensity (Dataset 1, GEO GSE74846) and were among those genes that modestly increased (OGA/WT ratio 1.0 –1.5-fold, enrichment score of 12.55) (Fig. 1, *c* and *d*). Fig. 1*d* also shows that the genes that most dramatically increase following OGA knockdown (1.5–2.25-fold enrichment) are those associated with protein degradation and steroid hormone activation. These data suggest that *O*-GlcNAc cycling is more dynamic on particular regions of chromatin. Therefore, chromatin response to the loss of OGA is not global, rather gene specific. Further bioinformatics analysis of ChIP-chip data were also performed by "two-sample analysis" as described under "Experimental Procedures." This analysis revealed interesting correlations between the *O*-GlcNAc and the other ChIP-chip datasets (Table 1, Dataset 1, GEO GSE74846). In agreement with the previously reported *O*-GlcNAc modification of Ph (6, 7), we found that 93% of Pho-occupied regions are also occupied by *O*-GlcNAc (Table 1, row 1, column C). Knockdown of OGA resulted in an increase, such that 96% of Pho-occupied regions were co-occupied by *O*-GlcNAc (Table 1, row 1, column D). As expected, knockdown of OGT decreased Pho and *O*-GlcNAc co-occupancy to 62% (Table 1, row 1, column E). Although OGT RNAi dramatically reduced both the number and intensity of nearly all *O*-GlcNAc-occupied regions, 62% of the Pho sites still had residual *O*-GlcNAc even after knockdown. We interpret this finding to suggest that *O*-GlcNAc occupancy at Pho sites is rather stable, not requiring persistent OGT activity.

O-GlcNAc occupied sites were more abundant and were not restricted to the Pho sites. For example, when *O*-GlcNAc occupied regions were compared with Pho-occupied regions we found that only 78% of the *O*-GlcNAc-occupied regions were also positive for Pho (Table 1, row 3, column A) in control. This overlap dropped to 66% after OGA RNAi because new *O*-GlcNAc intervals appeared that were distinct from the Pho-occupied regions (Table 1, row 4, column A). Thus, roughly 34% of chromatin regions occupied by *O*-GlcNAc modified proteins that are not associated with the Pc group of repressor proteins following OGA RNAi. We interpret this finding to suggest that Pc is not the only protein complex to be *O*-GlcNAc

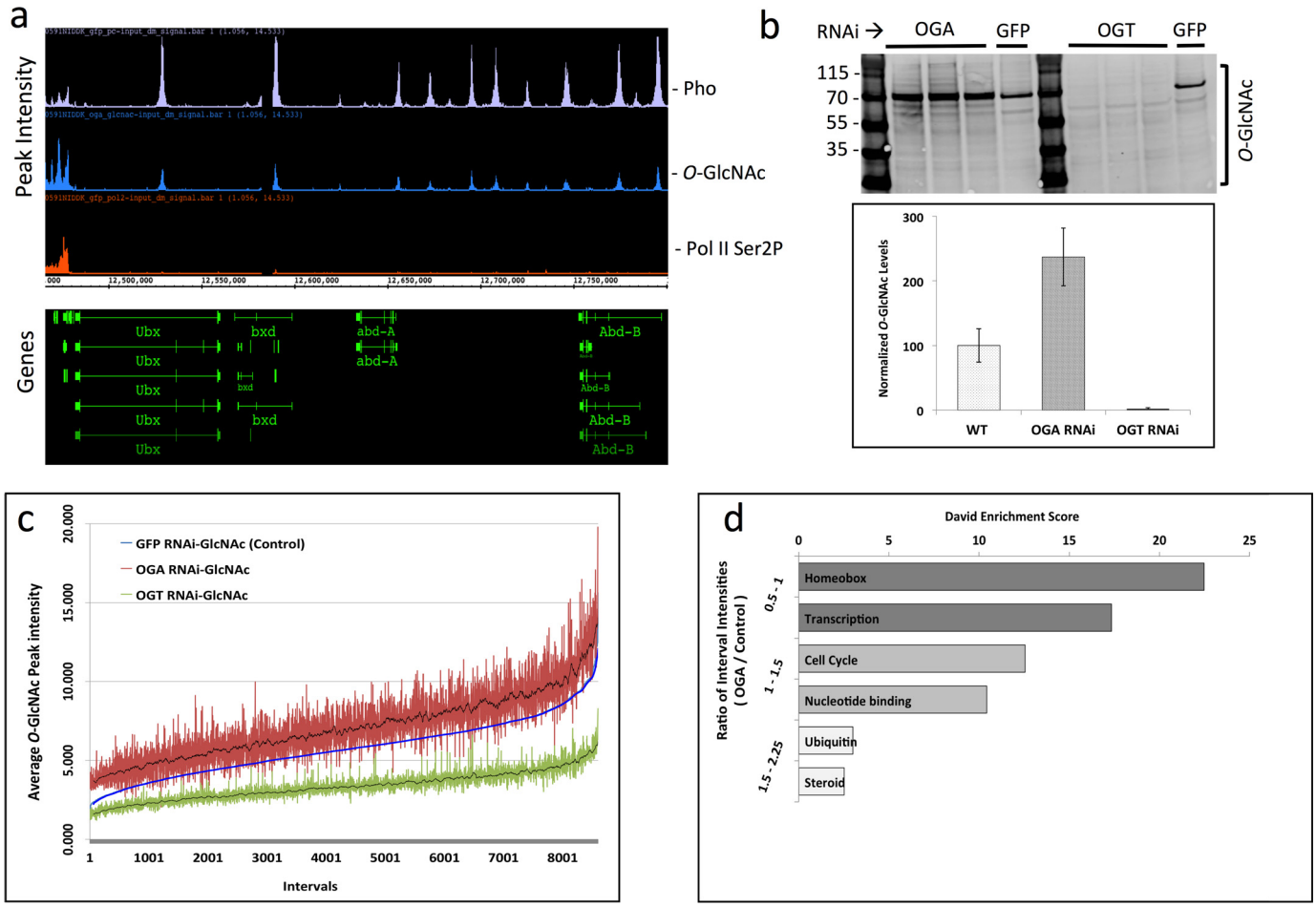

FIGURE 1. ***O*-GlcNAc cycling occurs at sites co-occupied by Polycomb group proteins on promoters of many transcriptionally silenced genes.** *a*, antibodies specific to *O*-GlcNAc, Pleiohomeotic (Pho), and RNA Pol II Ser2P were used for ChIP-chip analysis. *O*-GlcNAc and Pho marks overlap significantly at transcriptionally silenced regions. A representative region of the genome, chromosome 3 in the Bithorax cluster, including *abd-A* and *adb-B* is shown. Hox genes are occupied by Pho (*white*) and *O*-GlcNAc (*blue*) but lack significant accumulation of RNA Pol II Ser2P (*orange*, bottom). *b*, *O*-GlcNAc levels were detected following OGA RNAi and OGT RNAi in S2 cells. *O*-GlcNAc levels were increased ~2-fold following OGA RNAi compared with GFP RNAi. The *O*-GlcNAc signal was normalized to actin loading control. The graph represents average ± S.D. *c*, the *O*-GlcNAc peak intensities of each of ~8000 regions similar to those shown in *a* were plotted in increasing order of intensity. Peak intensities increased an average of 1.4-fold in OGA knockdown (*red*) cells, whereas intensities decreased to near background levels in OGT knockdown (*green*) cells compared with GFP control RNAi (*blue*). A 50-gene moving average for OGA and OGT knockdown is highlighted in *black*, with *blue* denoting a GFP (WT) control. *d*, the ratio of peak intensity observed for OGA to WT samples on the Affymetrix Genechip arrays was calculated for each of the roughly 8000 *O*-GlcNAc occupied chromatin sites. Those intervals that did not change significantly upon OGA knockdown (0.5–1.0) were examined bioinformatically using DAVID functional annotation clustering (42) and found to be 23-fold enriched for Hox genes and other transcriptional regulators ($p < 0.0001$). Intervals exhibiting an intermediate response to OGA knockdown were 10–12-fold enriched in genes associated with cell cycle and ATP utilization ($p < 0.0001$). Those showing the greatest change in intensity (1.5–2.5) between OGA and wild type showed a more modest 2–3-fold enrichment for genes associated with ubiquitin and steroid hormone response ($p < 0.001$).

TABLE 1

Correlations of chromatin occupancies of Pho, RNA Pol II Ser2P, and *O*-GlcNAc following GFP, OGT, or OGA RNAi in *Drosophila* S2 cells

ChIP-chip data for O-GlcNAc, Pho, and RNA Pol II Ser2P were statistically analyzed for co-enrichment with Affymetrix TAS software as described under "Experimental Procedures." Enrichment for each of the genomic regions on the chip in control, Pho, and RNA Pol II Ser2P datas were compared to *O*-GlcNAc data in control (GFP RNAi), OGA RNAi, and OGT RNAi cells for their presence on the same region of the genome. The table represents the percentage of the overlap between each of the statistically significant signals.

		A: GFP-RNAi, Pho	B: GFP- RNAi, Pol II Ser2P	C: GFP-RNAi, *O*-GlcNAc	D: OGA-RNAi, *O*-GlcNAc	E: OGT-RNAi, *O*-GlcNAc
1	GFP RNAi, Pho	100.00%	69.00%	93.06%	96.57%	62.20%
2	GFP RNAi, Pol II Ser2P	63.57%	100.00%	70.36%	79.70%	44.32%
3	GFP RNAi, *O*-GlcNAc	78.65%	63.66%	100.00%	98.03%	52.46%
4	OGA RNAi, *O*-GlcNAc	66.29%	59.20%	79.70%	100.00%	41.93%
5	OGT RNAi, *O*-GlcNAc	98.02%	73.71%	100.00%	99.83%	100.00%

modified by OGT on chromatin (Table 1). Moreover, we found 70% of RNA Pol II Ser2P occupied active chromatin regions were also occupied by *O*-GlcNAc (Table 1, row 2, column C). This striking overlap between *O*-GlcNAc and RNA Pol II Ser2P raised the possibility that the *O*-GlcNAc metabolism may directly influence transcription by acting at sites of active RNA Pol II elongation.

To analyze the affect of *O*-GlcNAc and RNA Pol II Ser2P chromatin co-occupancy on transcription, we utilized robust a Affymetrix analysis whole-genome *Drosophila* microarray fol-

TABLE 2

DAVID clustering analysis of gene expression changes upon OGT and OGA RNAi

The change in gene expression for OGT RNAi- or OGA RNAi-treated *Drosophila* S2 cells compared to control (GFP RNAi) was performed. The genes that increased or decreased more than 1.5-fold were analyzed by the DAVID Functional Annotation tool. The expression of nearly 300 genes was changed upon OGT RNAi treatment and the most enriched pathways are noted. To examine the changes in gene expression upon OGA RNAi treatment, we lowered the threshold for gene expression to 1.2-fold, and saw an increase in pathways depicted in the table. No gene other than OGA was downregulated. All clustering analysis yielded a p value < 0.05 for each annotation and enrichment score noted.

Treatment	Annotation	Fold-enrichment	Number of genes	p value
OGT-RNAi up-regulated[a]	Instar larval or pupal morphogenesis	2.6	15	8.29E-05
	Sugar/inositol transport	2.0	4	8.60E-04
	Behavior	1.9	15	7.39E-04
	Neurotransmitter transport	1.8	7	0.00455
	Adult behavior	1.7	7	0.00358
OGT-RNAi down-regulated	Cell cycle	2.3	18	1.73E-05
	Chromosome	1.7	8	0.00407
OGA-RNAi up-regulated[b]	Regulation of cell morphogenesis	1.9	5	0.00125
	Female gamete generation	1.9	10	2.16E-04
	Actin cytoskeleton organization	1.7	5	0.00245
	Posttranscriptional regulation of gene expression	1.6	5	0.00154
	Regulation of growth	1.5	3	0.00597
OGA-RNAi down-regulated	OGA	NA[c]	1	NA

[a] OGT RNAi: 1.5-fold up- and down-regulated, p value <0.05.
[b] OGA RNAi: 1.2-fold up- and down-regulated, p value <0.05.
[c] NA, not applicable.

lowing OGT or OGA knockdown. We found that the expression of genes related to development, cell cycle, and metabolism were affected (Table 2) when *O*-GlcNAc levels were perturbed by RNAi. The complete list of deregulated genes can be found in Dataset 2 (GEO GSE74846). We were surprised to find that whereas knockdown of OGT yielded deregulation of 321 unique genes more than 1.5-fold, knockdown of OGA yielded down-regulation of only OGA expression when the same stringency was applied (Table 2). Because RNAi was demonstrated to be effective at silencing both OGA and OGT (see Fig. 1*b*) this finding suggests that active transcription was more sensitive to loss of OGT than OGA. Upon further examination with reduced stringency, genes that were 1.2-fold up-regulated in OGA knockdown cells with $p < 0.05$ included those predicted by DAVID analysis (42) to be important for cell morphogenesis, oogenesis, and female gamete generation, suggesting that development or oogenesis might be more sensitive to OGA in flies. This possibility prompted us to examine the impact of loss of the *oga* gene in the context of *Drosophila* embryogenesis and development in the intact animal.

Generation of OGA Knock-out Flies—To examine the impact of blocked *O*-GlcNAc cycling *in Drosophila* development we generated $oga^{del.1}$ flies by P-element excision using a P-element insertion line generated in the gene disruption project (43). The P-element was originally inserted ~100 bp upstream of the *oga* ATG start site. Excision removed 657 bp through the *oga* gene including the promoter, first exon, and a portion of the second exon (Fig. 2*a*). The deletion removed 171 amino acids at the N terminus of the protein sequence, corresponding to over half of the predicted *O*-GlcNAcase domain including nearly all of the catalytically important residues (Fig. 2*b*). In addition, transcript levels were monitored by RT-PCR and reduced to near zero (%) at the deleted locus (data not shown). The rest of the gene is transcribed at levels comparable with WT (data not shown), therefore it is possible that a truncated protein containing an intact C-terminal domain including the pseudo-histone acetyltransferase domain could still be made in $oga^{del.1}$ mutants. In animals lacking *O*-GlcNAcase activity, we expected an increase in the levels of *O*-GlcNAc-modified proteins. Indeed, we observed a significant (~6-fold) increase in protein *O*-GlcNAcylation for $oga^{del.1}$ mutant fly extracts compared with heterozygote ($oga^{del.1}$/TM6) or wild type (WT) fly extracts (Fig. 2*c*) as reflected by *O*-GlcNAc band intensities. UAS-driven OGA RNAi led to a more modest increase in *O*-GlcNAc levels than the deletion strain (Fig. 2*c*, *right panels*). In control rescue experiments, ectopic expression of UAS-OGA in $oga^{del.1}$ mutant flies using the actin-Gal4 promoter restored *O*-GlcNAc levels to WT (w^{1118}) levels (Fig. 2*d*). To determine the level of *O*-GlcNAcase enzyme activity in $oga^{del.1}$ flies, we analyzed ovary protein extracts for *in vitro* OGA activity. $oga^{del.1}$ mutant ovary protein extracts displayed very little *O*-GlcNAcase-specific enzyme activity when compared with WT (Fig. 2*e*) with residual activity attributed to additional hexosaminidases and chitinases present in the extract (39). Thus, we conclude that $oga^{del.1}$ animals lack significant *O*-GlcNAcase activity. Phenotypically, homozygous $oga^{del.1}$ mutants were viable and fertile. The mutants showed a semi-penetrant oogenesis defect that was rescued by overexpressing OGA under actin-Gal4 or ovary-specific nanos-Gal4 promoter to restore normal cycling of *O*-GlcNAc (supplemental Fig. S1). However, fertility was also normal when $oga^{del.1}$ mutants were crossed to two different *oga* deficiency lines. The deficiency lines are missing at least 30 genes near the "NK" cluster of homeotic genes in *Drosophila* including *oga*. There are numerous possible interpretations of our findings. First, the dosage of truncated OGA protein or mRNA may be important for the defective oogenesis phenotype. Second, the dosage of another gene that is missing in the deficiency line may be important for the oogenesis defect in $oga^{del.1}$ mutants. We are currently testing these and other possibilities.

Polytene Chromosomes Reveal Genome-wide Distribution of Chromatin Modifiers in O-GlcNAc Cycling Mutants—Polytene chromosomes allow visualization and global analysis of chromatin-associated factors in *Drosophila.* This allowed us to extend our ChIP-Chip findings on S2 cells to chromosomes derived from genetically defined *Drosophila* larvae. We first

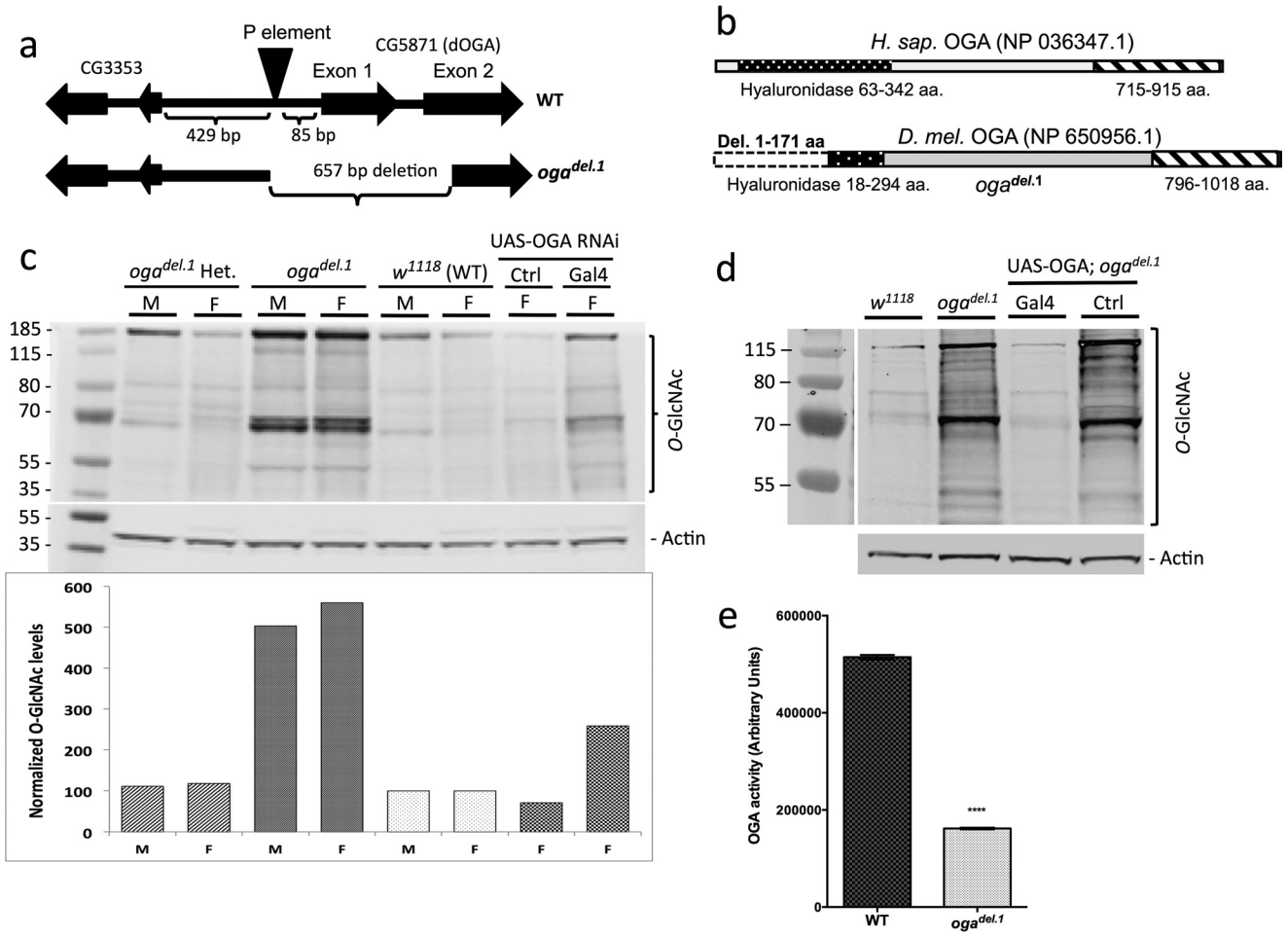

FIGURE 2. ***oga* deletion mutant flies have increased protein *O*-GlcNAcylation.** *a,* the P element that is located upstream of the *oga* gene was excised by P element excision. The excision removed 657 bp into *oga* removing the transcription start site and a portion of the second exon. *b*, the deletion removed the N-terminal 171 amino acids into the predicted *O*-GlcNAcase domain of the protein. *c, oga*$^{del.1}$ males or females both display an increase in the amount of *O*-GlcNAc-modified proteins compared with WT or heterozygotes. *O*-GlcNAc (RL2) and actin are loading controls. Comparison of *O*-GlcNAc levels after normalization to actin loading control levels in the bar graph shows that *oga* deletion mutants have ~6-fold more *O*-GlcNAc levels than WT. UAS-driven OGA RNAi showed a more modest silencing of OGA as evidenced by the partial increase in *O*-GlcNAc levels (*right panels*). *d,* ectopic expression of OGA (UAS-OGA) with actin-GAL4 promoter restores *O*-GlcNAc levels similar to WT levels in *oga*$^{del.1}$ mutant background. *M,* males; *F,* females. *e, oga*$^{del.1}$ ovaries display diminished *O*-GlcNAcase activity measured by fluorogenic OGA enzymatic assay. Data represent mean ± S.E. (****, $p < 0.0001$).

examined the genome-wide distribution of *O*-GlcNAc upon disruption *O*-GlcNAc cycling in polytene chromosomes in WT, *oga*$^{del.1}$, and *ogt* (*sxc*) mutant lines. The numbers of *O*-GlcNAc positive sites and relative staining intensity increased significantly in the *oga*$^{del.1}$ mutant when compared with WT and *O*-GlcNAc bands are absent in the *ogt*(*sxc*) mutants (Fig. 3). We then colocalized these *O*-GlcNAc bands with other relevant markers of transcriptional activity. As shown in Fig. 4, we found *O*-GlcNAc was present at a limited number of discrete sites on WT polytene chromosomes compared with elongating RNA Pol II Ser2P, which was much more abundant (Fig. 4, *left panels, w*^{1118}). The number and intensity of *O*-GlcNAc positive bands increased in *oga*$^{del.1}$ mutant polytenes and the overlap with RNA Pol II Ser2P also was demonstrably increased (Fig, 4, *middle panels*, *oga*$^{del.1}$).

In contrast to the findings with RNA Pol II Ser2P, the major *O*-GlcNAc sites co-localized with Pc (Fig. 4, *middle panel*, *w*^{1118}) and Pho (supplemental Fig. S2) in WT flies confirmed the high degree of overlap observed in ChIP-chip results in S2 cells (Fig. 1 and Table 1). In the *oga*$^{del.1}$ strain many more *O*-GlcNAc bands appeared that were not coincident with Pc (Fig. 4, *right panel*, *oga*$^{del.1}$). This suggests that *O*-GlcNAc cycling normally occur at those sites.

These findings, and our previously described ChIP-chip analysis showed that many more *O*-GlcNAc occupied regions were free from Pho and coincident with RNA Pol II Ser2P upon OGA knockdown. The presence of *O*-GlcNAc at sites of active transcriptional elongation prompted us to question whether Pho-independent *O*-GlcNAc-enriched chromatin regions were co-occupied by Trithorax or Compass group members. *Drosophila* TRX, ASH1, and SET1 are all capable of methylating histone 3 (H3) thereby opening chromatin to allow for active transcription. TRX monomethylates H3K4, whereas SET1 and ASH1 are responsible for trimethylation of H3K4 and dimethylation of H3K36, respectively (44). After observing the dramatically increased chromatin occupancy of *O*-GlcNAc on *oga*$^{del.1}$ mutant polytenes in comparison to WT (Fig. 4), we co-stained polytene chromosomes of *oga*$^{del.1}$ mutants with *O*-GlcNAc and antibodies against each of the Trithorax members: TRX, ASH1, or Compass member SET1. In WT, we observed that a limited

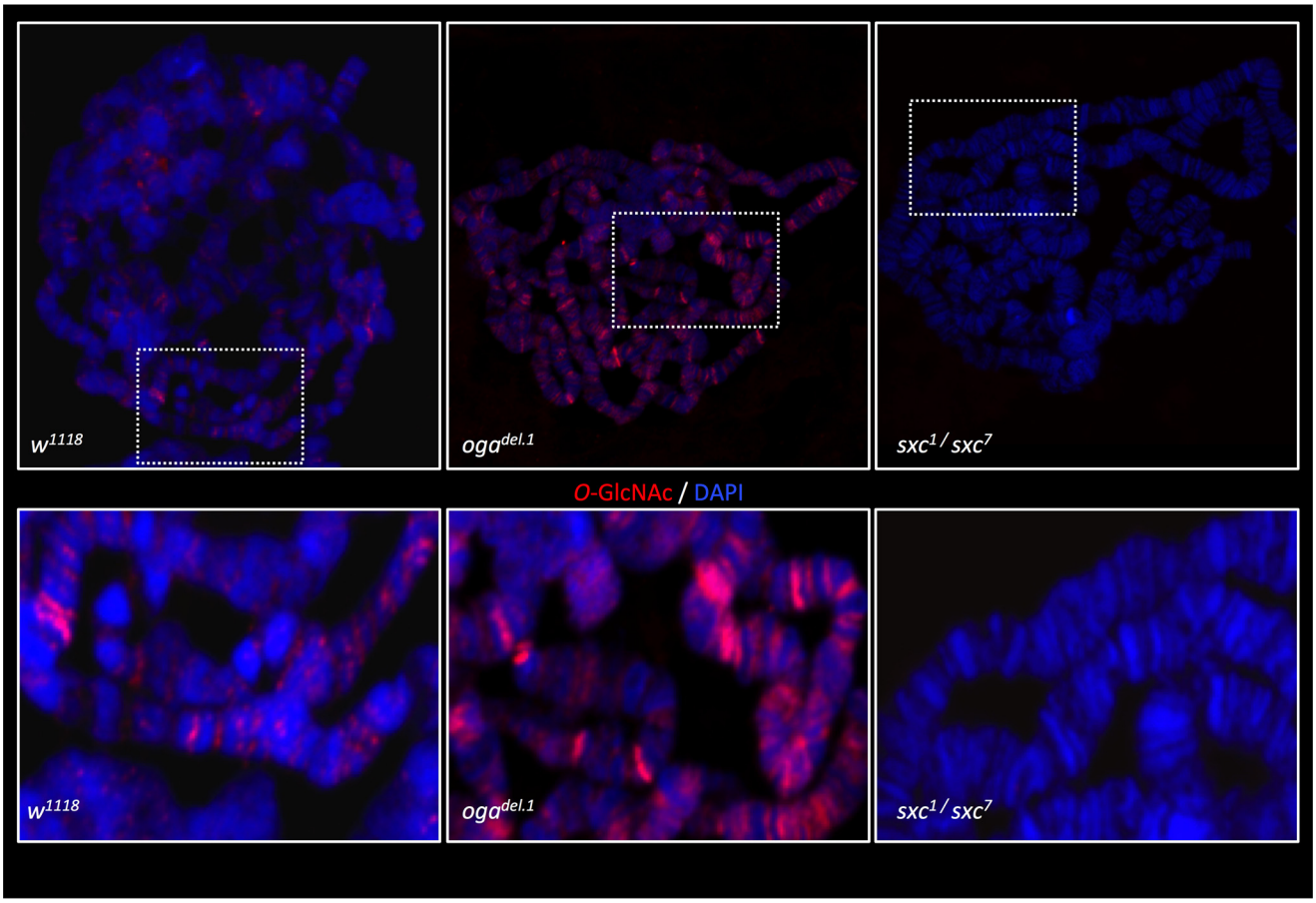

FIGURE 3. ***O*-GlcNAc levels and number of detected bands increased in $oga^{del.1}$ mutant polytene chromosomes.** Polytene chromosomes were prepared from WT (w^{1118}), *oga* ($oga^{del.1}$), and *ogt* (sxc^1/sxc^7) mutants. *O*-GlcNAc signal level (*red*) and number of bands increased in $oga^{del.1}$ mutants. *ogt* (sxc^1/sxc^7) mutant polytene is used as negative control for *O*-GlcNAc staining. *Bottom panel* shows the enlarged images of dashed boxes in the *upper panel* for a closer look at the banding pattern on polytenes.

number of bands co-stained with *O*-GlcNAc and each of these proteins (Fig. 5). Strikingly, we observed more bands corresponding to each of these proteins on polytene chromosomes of $oga^{del.1}$ mutants. Despite the increases in *O*-GlcNAc at sites associated with these proteins in the $oga^{del.1}$ mutants, not all the bands stained with TRX, ASH1, or SET1 were co-stained with *O*-GlcNAc.

ASH1, SET1, and TRX Histone Methyltransferases Are O-GlcNAc Modified—Direct *O*-GlcNAc modification of TRX, ASH1, and SET1 could potentially alter their stability, activity, or chromatin binding efficiency, which could lead to inappropriate gene expression in $oga^{del.1}$ flies. To examine whether these Trithorax group and Compass proteins were modified directly by *O*-GlcNAc, we immunoprecipitated each from ovary extracts and probed for *O*-GlcNAc. All three proteins showed detectable levels of *O*-GlcNAc modification in $oga^{del.1}$ ovary extracts, although none of them were detectable in WT. TRX has been shown to exist in as many isoforms that are separable on SDS-PAGE (45). We saw *O*-GlcNAcylation of these same isoforms for TRX following immunoprecipitation (Fig. 6). Importantly, BRE1, which is thought to modulate SET1 activity (46), did not show an increase in *O*-GlcNAc modification under the same IP conditions. These findings suggest that the *O*-GlcNAc modification of TRX, ASH1, and SET1 is normally at substoichiometric levels and increases when *O*-GlcNAcase activity is eliminated (Fig. 6). Furthermore, our results underscore that the $oga^{del.1}$ animals generated herein provide an excellent tool to: 1) identify proteins that are *O*-GlcNAc modified and 2) examine the consequences of the post-translational modification on protein stability and function *in vivo*.

We next postulated that the irreversible *O*-GlcNAcylation of these three histone methyltransferases could change their activity thereby interfering with the proper spatiotemporal expression of their target genes. To test this theory, we examined H3 modifications in $oga^{del.1}$ ovaries by immunoblotting and noted no significant changes in the H3 methylations analyzed (Fig. 7*a*). We suggest that subtle chromatin methylation differences between WT and $oga^{del.1}$ would be hard to detect in whole ovary extracts because the ovary contains many different cell types including stem, nurse, oocyte, somatic cells, all of which are constantly developing to produce the mature egg. To examine possible cell type-specific H3 modification differences that might be present, we generated germline chimeras (Fig. 7*b*) using a FRT/FLP mosaic system (36), in which we were able to detect individual cells as $oga^{del.1}$ mutant (GFP negative) or WT/heterozygote (GFP positive). Quantitation of the levels of H3 methylation in the germline stem cells show a slight decrease, which did not reach statistical significance between the $oga^{del.1}$ and adjacent wild type or heterozygous cells. We also observed no difference in H3 methylation in somatic fol-

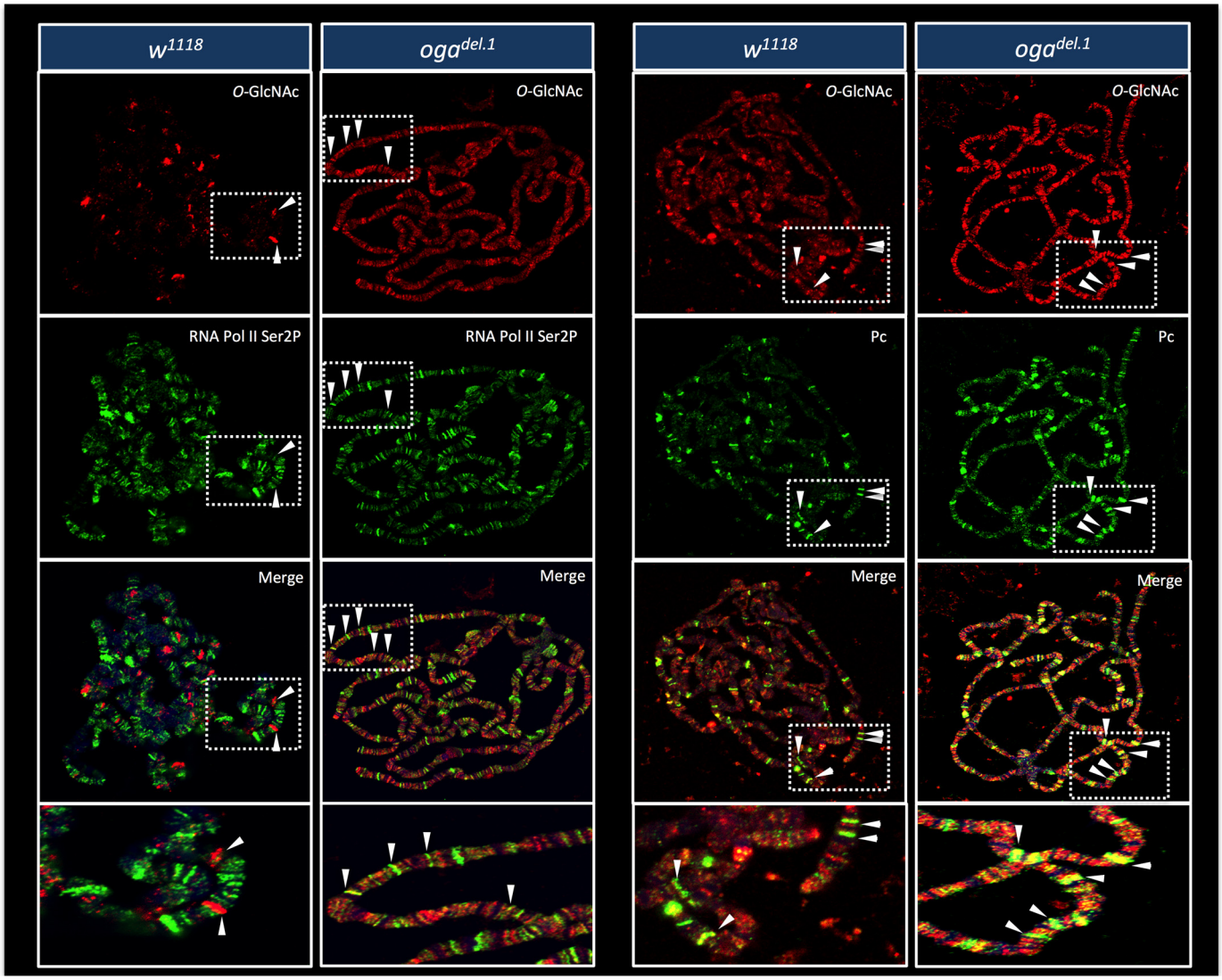

FIGURE 4. **Blocked *O*-GlcNAc cycling alters the distribution of *O*-GlcNAc sites with respect to elongating RNA Pol II and sites of Pc repression.** Polytene chromosomes were prepared from WT (w^{1118}) and *oga* ($oga^{del.1}$) mutant flies. The chromosomes were stained with both anti-*O*-GlcNAc antibody and RNA Pol II Ser2P (elongating RNA Pol II) or Pc. The number of *O*-GlcNAc and Pol II Ser2P co-localized bands increased in $oga^{del.1}$ (*left panel*, w^{1118} *versus* $oga^{del.1}$). *O*-GlcNAc and Pc shows co-localized polytenes (w^{1118}, *right panel*). Many more *O*-GlcNAc-specific bands were separate from Pc bands (*right panel*, w^{1118} *versus* $oga^{del.1}$). (Select co-localized bands are shown with *arrowheads*. *Lower panel* is a blow up of the *dashed squares* to clearly define bands on the polytenes. *O*-GlcNAc sites are distinct from RNA Pol II Ser2P, but largely coincident with Pc on polytene chromosomes. Increased *O*-GlcNAc sites resulting from the $oga^{del.1}$ mutant show increased coincidence with RNA Pol II Ser2P and appear at sites distinct from Pc. RNA Pol II Ser2P, and Pc (*green*), *O*-GlcNAc (*red*) and DAPI (*blue*) are shown. Co-stained bands appear as *yellow*.

licular cells between these genotypes. These findings are reminiscent of *ogt* mutants, which also did not show any change in H3K27me3 levels despite the fact that OGT is essential for Ph function and proper development (6, 7).

Gene Expression Is Deregulated in $oga^{del.1}$ Ovaries—Detection of ASH1, TRX, and SET1 as new *O*-GlcNAc targets raised the possibility of gene expression changes that may occur as a result of irreversible *O*-GlcNAcylation during development and differentiation in a specific tissue or cell type. These cell type-specific changes may not have been detected in S2 cells following OGA RNAi. To address that possibility, we chose a small group of highly *O*-GlcNAc-enriched genes from the ChIP-chip dataset (GEO database GSE74846, Dataset 1) and analyzed the expression of oogenesis-related (HTS, Capicua, PKA-C1, sxl, bam, and bazooka) and cell cycle-related (bam, bazooka, HCF, embargoed) genes by RT-PCR in ovaries, where there constant development and differentiation occur. Interestingly, the expression of oogenesis-related genes did not change, but cell cycle-related HCF and embargoed genes were up-regulated in $oga^{del.1}$ mutant ovaries (Fig. 8). Importantly, not all the cell cycle genes we analyzed had differential expression in $oga^{del.1}$ mutants. These data suggest that the expression of only a subset of genes were affected in $oga^{del.1}$ mutants.

Discussion

Dynamic O-GlcNAc Cycling Is Highly Regulated and Occurs at All But a Small Subset of the Thousands of Genomic Sites in Drosophila—Disturbances in proper *O*-GlcNAcylation can result in defects in embryonic development and complications including tumor formation and insulin resistance (47, 48). By

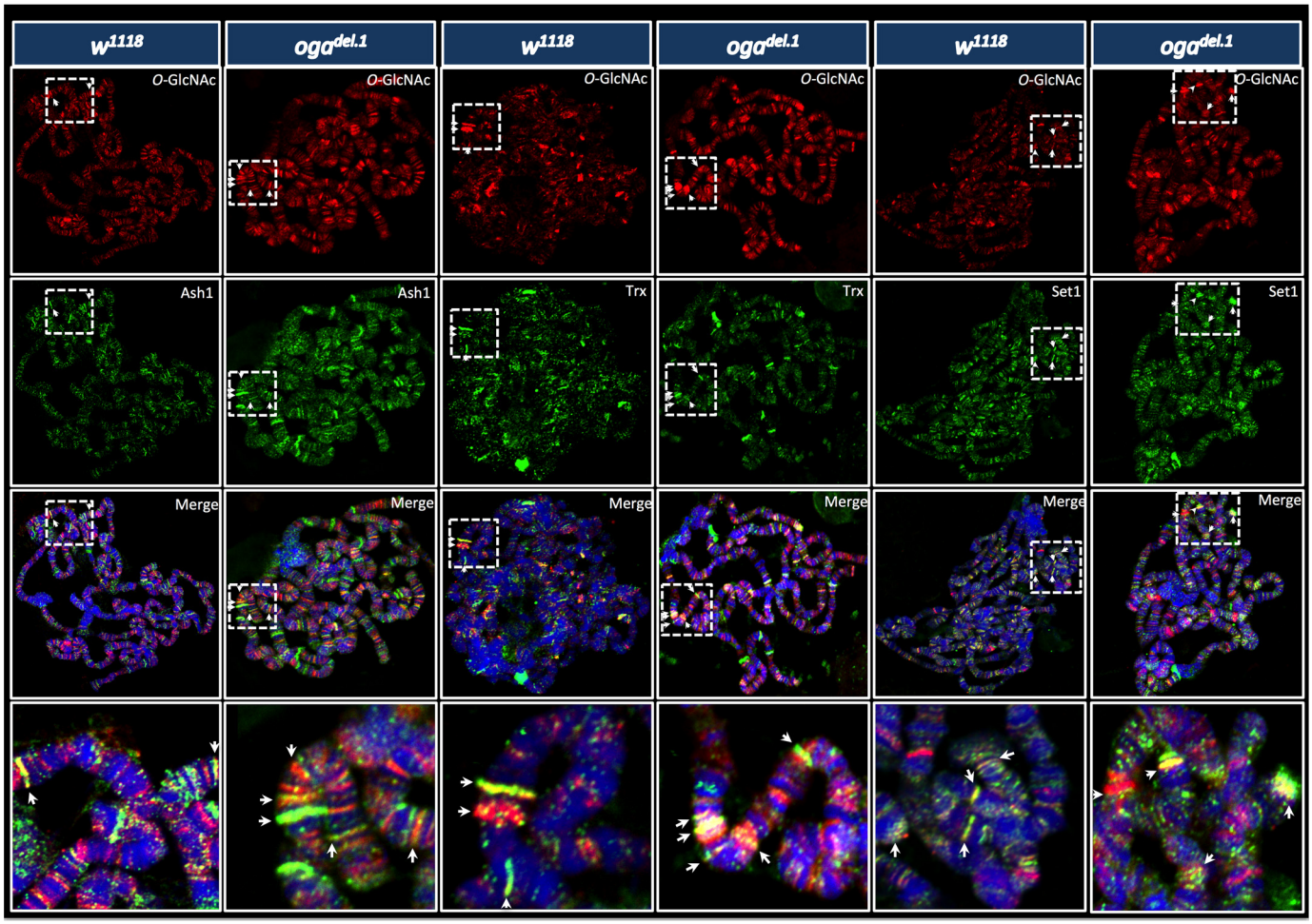

FIGURE 5. **Increased co-localization of ASH1, SET1, and TRX with *O*-GlcNAc on *oga*$^{del.1}$ mutant polytene chromosomes compared with wild type.** Polytene chromosomes prepared from WT (w^{1118}) and *oga* mutant (*oga*$^{del.1}$) animals were co-stained for TRX, ASH1, or SET1 along with *O*-GlcNAc. More bands corresponding to each of these proteins were observed on polytenes of *oga*$^{del.1}$ compared with w^{1118} (*green* signal for each protein). A subset of ASH1, TRX, of SET1 positive bands were also stained with *O*-GlcNAc (*orange-yellow*). ASH1, TRX, or SET1, (*green*), *O*-GlcNAc (*red*), and DAPI (*blue*) are shown. *Bottom panel* is a blow-up of the *marked squares* to show bands and co-staining more clearly. Representative co-stained (*yellow*, *orange*) bands are shown with *arrows*.

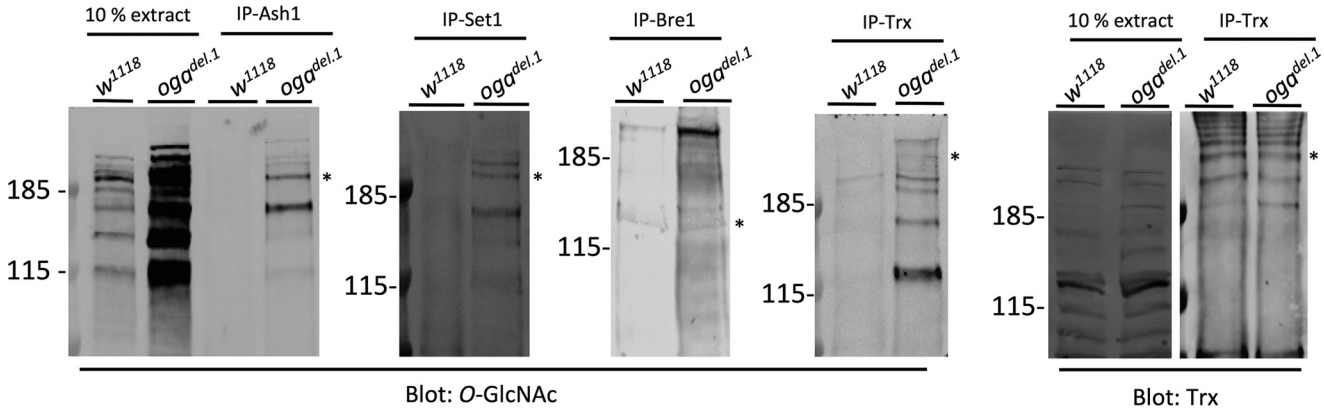

FIGURE 6. **ASH1, SET1, and TRX are *O*-GlcNAc modified in *oga*$^{del.1}$ ovaries.** Equal amounts of ovary protein extracts were used for immunoprecipitation with TRX, ASH1, SET1, or BRE1 antibodies and run on SDS-PAGE gel. Membranes were immunoblotted for RL2 anti-*O*-GlcNAc antibody. ASH1 (~246 kDa), SET1 (~188 kDa), and TRX (~400 kDa) are detected by anti-*O*-GlcNAc antibody (RL2) in *oga*$^{del.1}$ ovary extracts compared with WT. Bre1 (~115 kDa) was not *O*-GlcNAc enriched in *oga* mutants under the same IP conditions. *O*-GlcNAc and the TRX blot using 10% extract for IPs are shown. Predicted molecular weight of each protein is indicated with an *asterisk*.

ChIP-chip analysis, we noted several key features of *O*-GlcNAc chromatin occupancy upon disruption of either OGT or OGA expression in *Drosophila* S2 cells. We observed ~8000 regions of the *Drosophila* genome where *O*-GlcNAc resides with a significant overlap with RNA Pol II Ser2P. The bulk of these active regions have a single interval associated with each gene, often at promoters. Over 7500 of these intervals increase in intensity (average 1.4-fold) upon OGA knockdown. A much smaller sub-

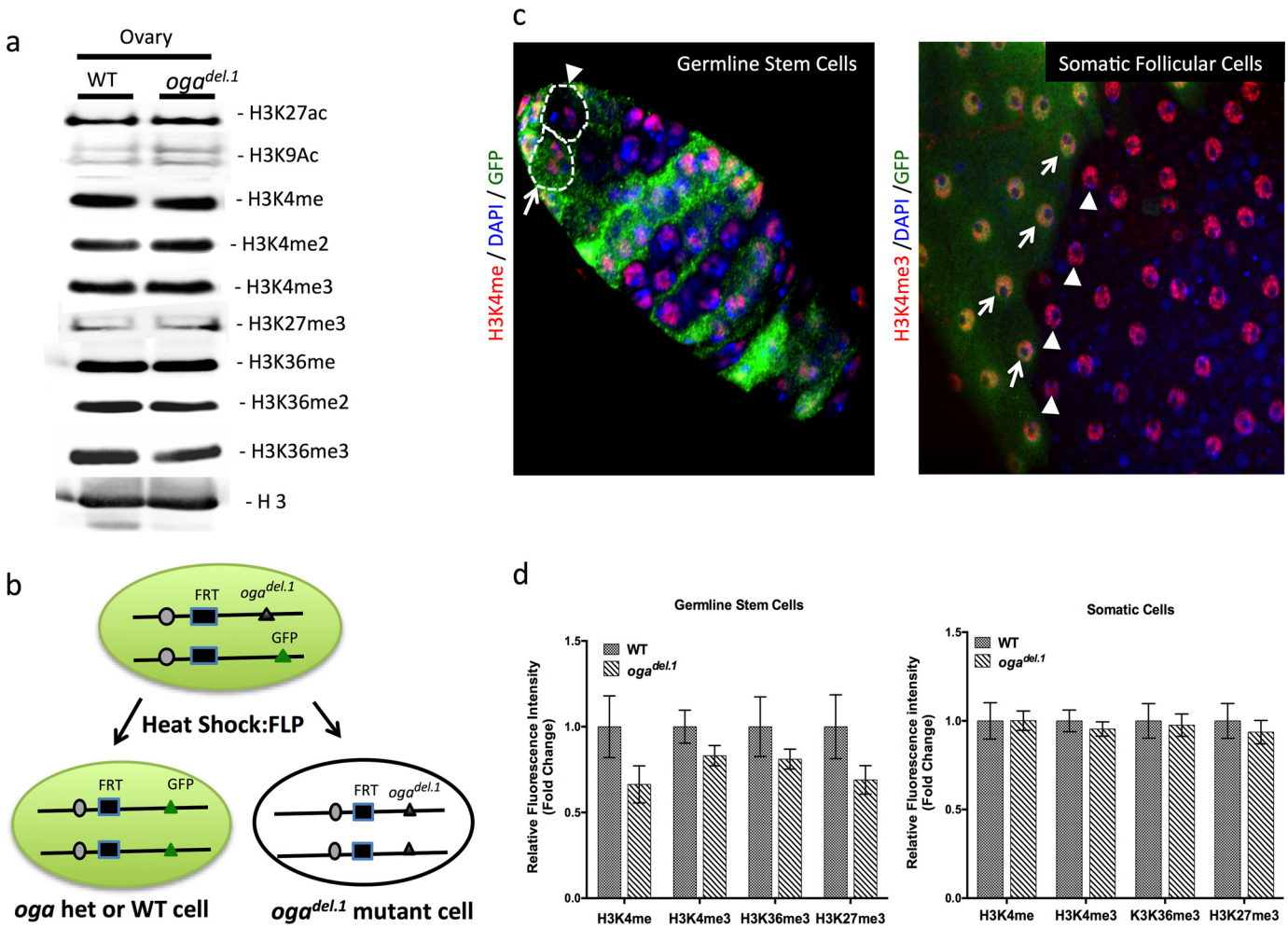

FIGURE 7. **H3 modifications were not altered in *oga*$^{del.1}$ ovaries compared with WT.** *a,* histone 3 modifications of WT and *oga*$^{del.1}$ ovary extracts were analyzed by immunoblotting. No difference in signal was observed for the 9 marks analyzed. *b,* cell-specific changes in histone marks were examined by generating *oga*$^{del.1}$ germline mosaics. Schematic representation of the generation of mosaics. *c,* H3K4me, H3K4me3, H3K36me3, and H3K27me3 histone marks were compared between the *oga*$^{del.1}$ mutant (GFP negative) *versus* neighboring WT or heterozygote cells (GFP positive) in ovary by immunofluorescence. Representative images were stained for GFP (*green*), DAPI (*blue*), and H3K4me (*red*) in ovary germline stem cells (*left panel*, *dashed lines*) and H3K4me3 (*red*) in somatic cells (*right panel*). WT cells are denoted by an *arrow* and *oga*$^{del.1}$ cells are denoted by an *arrowhead*. Signals for each histone mark was normalized to DAPI for each cell; the normalized signal from *oga*$^{del.1}$ cells were then compared with the normalized signal of neighboring WT cells and plotted as fold-change compared with WT (*d*). Germline stem cells (*left graph*) and somatic follicular cells (*right graph*) showed no statistical difference between *oga*$^{del.1}$ and neighboring WT or heterozygote cells. Data represent mean ± S.E.

set (~500 genes) either slightly decrease or stay constant upon OGA depletion (ratio of 0.5–1.0). Hox genes and other transcriptional regulators are highly over-represented in these genes that change little in response to OGA knockdown. These are also the major sites of Polycomb repression in *Drosophila.* The finding that these chromatin regions are insensitive to OGA loss of function is consistent with a model in which these domains are normally unavailable to OGA because of chromatin structure or the lack of a histone signature to recruit OGA to those regions. Intriguingly, the genes showing most dramatic elevation of *O*-GlcNAc chromatin occupancy upon OGA depletion were those associated with protein degradation (ubiquitin), and rapid gene activation (steroid hormone response).

OGA Loss of Function Differs from OGT Loss of Function in Both Phenotype and Gene Expression Changes—Whereas we expected to see a significant number of gene expression changes by whole genome microarray based on the overlap between *O*-GlcNAc and RNA Pol II Ser2P, we observed only few changes upon OGA knockdown in S2 cells. The knockdown of OGA was demonstrated to be highly efficient (Fig. 1) although we cannot exclude the possibility that it did not reach the threshold required for major changes in gene expression. The knockdown did achieve elevation of total *O*-GlcNAc levels and increase in *O*-GlcNAc occupancy at sites across the genome. The minor changes in gene expression after OGA knockdown raises the possibility that a subset of genes may be deregulated in a specialized cell type, or in a tissue that is sensitive to changes in *O*-GlcNAc levels. Alternatively, redundant bypass mechanisms may act to limit the impact on transcription. It should also be noted that loss of OGA had a more modest effect on transcription than loss of OGT in our previous analysis in *C. elegans* (19).

Both *Ogt* (49) and *Oga* (50, 51) are essential for normal development in mice, and *ogt* is required for proper body development in *Drosophila* (9). We hypothesized that an *oga* knock-out

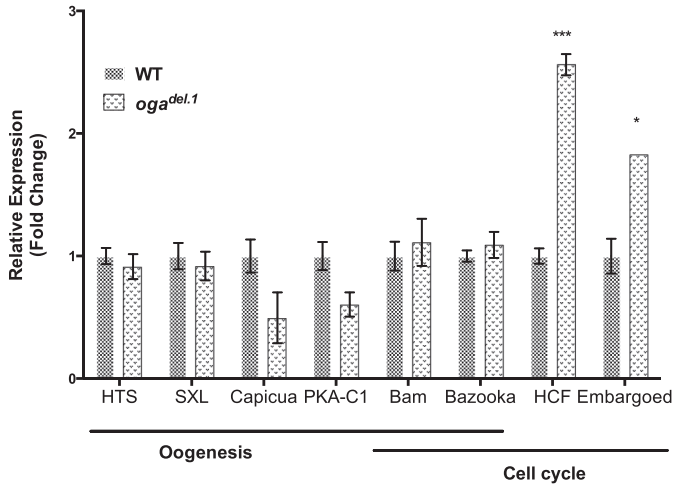

FIGURE 8. **The expression of cell cycle-related genes HCF and embargoed are increased in *oga*$^{del.1}$ ovaries.** The expression of oogenesis and cell cycle-related genes in 5-day-old female ovaries was measured by RT-PCR. Expression of the each gene was normalized to ribosomal RNA. Gene expression of *oga*$^{del.1}$ mutants were then compared with WT and plotted as fold-change to analyze the difference. Cell cycle-related HCF and embargoed showed a nearly 2-fold increase in *oga*$^{del.1}$ mutants, whereas there was no difference in the expression of oogenesis-related genes between *oga*$^{del.1}$ and WT ovaries. *Error bars* represent mean ± S.E. (*, $p < 0.05$; **, $p < 0.0005$).

in *Drosophila* would have similar homeotic defects. To our surprise, *oga* knock-out flies are viable with no visible homeotic transformations.

O-GlcNAc Cycling Occurs at Sites Associated with Polycomb and Trithorax Complexes—Our phenotypic analysis suggested that Pc repression is not disturbed in *oga* mutants. Polytene chromosomes isolated from WT, *ogt(sxc)*, and *oga* mutants were used to further examine the association of *O*-GlcNAc with polycomb and other chromatin modifiers. Polytenes from WT flies exhibited a banding pattern largely coincident with Pc and Pho; no *O*-GlcNAc-specific bands were detectable in polytenes prepared from *ogt(sxc)*. *oga* deletion flies showed a polytene banding pattern with many more bands with higher overall intensity. These new bands were in addition to those seen in wild type. These new bands appearing on polytenes derived from *oga* deletion flies were shown to significantly overlap with members of the Trithorax group (TRX, ASH1) and Compass group (SET1) of transcriptional activators. Interestingly, only a subset of the sites stained positive for TRX, ASH1, or SET1 were also stained positive for *O*-GlcNAc, suggesting that a subset of their target genes were sensitive to *O*-GlcNAc levels. We then examined whether epigenetic activators in the TRX or Compass complexes were *O*-GlcNAc modified. We selected ovary tissue for use in our experiments as *Drosophila* ovaries have a high number of germ cells that are constantly differentiating from a stem cell to a mature egg making them ideal to study epigenetic machinery. Indeed, we found that TRX, ASH1, and SET1 are *O*-GlcNAcylated in *oga*$^{del.1}$ ovaries. However, there were no global changes in the levels of histone modifications these enzymes perform. We then wondered whether this would result in any gene expression changes and selected to analyze a small set of genes whose promoters were highly *O*-GlcNAc modified in ChIP-chip analysis of S2 cells. Of the eight genes we analyzed, only the expression of HCF and embargoed were changed in *oga*$^{del.1}$ mutant ovaries supporting our hypothesis that the expression of a specific subset of genes in a specific cell or tissue type are likely to be affected by irreversible *O*-GlcNAc modification of TRX, ASH1, or SET1.

HCF, which is necessary for proper cell cycle progression, interacts with both Pc and Trx groups in *Drosophila* (52). Moreover, SET1 activity is regulated by HCF1 in mammals and HCF1 activity is regulated by *O*-GlcNAcylation (14, 27, 53). In light of our findings, we speculate that irreversible *O*-GlcNAcylation of SET1 and increased expression of HCF could alter cell cycle progression in a specific cell type in *oga*$^{del.1}$ mutants.

Regulation of gene expression by Pc group is different in male and female germlines in *Drosophila* (2). Recent work identified that PRC2 appears to control oogenesis by regulating the expression of cell cycle genes, whereas PRC1 members control sperm development (2). Similar to sex-specific germline regulation identified with the Pc complexes, TRX, ASH1, and SET1 could also display gender-specific phenotypes. Some evidence suggests that such regulation exists. For example, knockdown of SET1 causes an oogenesis defect, but does not affect neuronal development (54). It will be interesting to see whether *O*-GlcNAc plays a role in gender-specific or tissue-specific gene expression. Support for this idea comes from a study showing that OGT plays a critical role in neonatal epigenetic programming (55).

The O-GlcNAcase Mutant Fly as a Model for O-GlcNAc Cycling—The mammalian and fly OGA molecules show high sequence similarity and are likely to perform similar functions. Mammalian OGA (MGEA5) is suggested to play an *O*-GlcNAc independent role in activation of gene expression in that the pseudo-histone acetyltransferase domain of MGEA5 may play a role in gene activation (56). The deletion in *oga*$^{del.1}$ mutants spans the *O*-GlcNAcase catalytic domain but leaves the C-terminal pseudo-histone acetyltransferase domain intact. The fly system therefore should provide a valuable platform to examine the roles of the domains of OGA in performing its many functions.

Our study introduces viable *oga*$^{del.1}$ mutant flies as a valuable tool to study *in vivo* effects of increased *O*-GlcNAc levels. These mutants have greatly enhanced levels of chromatin-associated *O*-GlcNAc. Previous work has shown that RNA Pol II and other chromatin factors are substrates for *O*-GlcNAc on chromatin (15, 19, 40). Here we have shown that increased *O*-GlcNAc levels correlate with impairment of epigenetic modifications. We show that Trx members ASH1 and TRX, and Compass member SET1 histone methyltransferases are *O*-GlcNAc modified in ovaries and speculate that their stability or functions may be altered when they are irreversibly *O*-GlcNAcylated, which could ultimately change the expression of a subset of their target genes. The large number of potential *O*-GlcNAc targets on chromatin, and their increased modification upon interfering with *O*-GlcNAc cycling suggests a more general role for *O*-GlcNAcylation in stabilizing and activating epigenetic effectors.

Author Contributions—I. A., D. C. L., and J. A. H. planned and conducted experiments. I. A., J. A. H., and M. B. wrote the paper. D. C. L. and J. A. H. performed ChIP-chip experiments, M. B., I. A., and J. A. H. analyzed microarray and ChIP-chip data. K. R. H. performed the OGA assay.

Acknowledgments—We thank Drs. J. Leslie Brown, Judith A. Kassis, Kelly Ten Hagen, Michael Krause, and Mary Lilly for their helpful suggestions and assistance in carrying out the studies presented in this manuscript. We thank members of the Hanover lab for meticulously reviewing the manuscript. We thank Dr. Shilatifard for supplying antibodies as noted in the manuscript. We also acknowledge the Vienna Drosophila Resource Center (VDRC) for producing and supplying the numerous UAS-RNAi lines used in this study.

References

1. Chu, C. S., Lo, P. W., Yeh, Y. H., Hsu, P. H., Peng, S. H., Teng, Y. C., Kang, M. L., Wong, C. H., and Juan, L. J. (2014) *O*-GlcNAcylation regulates EZH2 protein stability and function. (2014) *Proc. Natl. Acad. Sci. U.S.A.* **111,** 1355–1360
2. Iovino, N., Ciabrelli, F., and Cavalli, G. (2013) PRC2 controls *Drosophila* oocyte cell fate by repressing cell cycle genes. *Dev. Cell* **26,** 431–439
3. Martinez, A. M., and Cavalli, G. (2006) The role of polycomb group proteins in cell cycle regulation during development. *Cell Cycle* **5,** 1189–1197
4. Dorighi, K. M., and Tamkun, J. W. (2013) The trithorax group proteins Kismet and ASH1 promote H3K36 dimethylation to counteract Polycomb group repression in *Drosophila*. *Development* **140,** 4182–4192
5. Schuettengruber, B., Martinez, A. M., Iovino, N., and Cavalli, G. (2011) Trithorax group proteins: switching genes on and keeping them active. *Nat. Rev. Mol. Cell Biol.* **12,** 799–814
6. Gambetta, M. C., Oktaba, K., and Müller, J. (2009) Essential role of the glycosyltransferase sxc/Ogt in polycomb repression. *Science* **325,** 93–96
7. Gambetta, M. C., and Müller, J. (2014) *O*-GlcNAcylation prevents aggregation of the polycomb group repressor polyhomeotic. *Dev. Cell* **31,** 629–639
8. Sinclair, D. A., Syrzycka, M., Macauley, M. S., Rastgardani, T., Komljenovic, I., Vocadlo, D. J., Brock, H. W., and Honda, B. M. (2009) *Drosophila* *O*-GlcNAc transferase (OGT) is encoded by the Polycomb group (PcG) gene, super sex combs (sxc). *Proc. Natl. Acad. Sci. U.S.A.* **106,** 13427–13432
9. Ingham, P. W. (1984) A gene that regulates the bithorax complex differentially in larval and adult cells of *Drosophila*. *Cell* **37,** 815–823
10. Hanover, J. A., Krause, M. W., and Love, D. C. (2010) The hexosamine signaling pathway: *O*-GlcNAc cycling in feast or famine. (2010) *Biochim. Biophys. Acta* **1800,** 80–95
11. Love, D. C., and Hanover, J. A. (2005) The hexosamine signaling pathway: deciphering the "O-GlcNAc code." *Sci. STKE* **2005,** re13
12. Bond, M. R., and Hanover, J. A. (2013) *O*-GlcNAc cycling: a link between metabolism and chronic disease. *Annu. Rev. Nutr.* **33,** 205–229
13. Zeidan, Q., Wang, Z., De Maio, A., and Hart, G. W. (2010) *O*-GlcNAc cycling enzymes associate with the translational machinery and modify core ribosomal proteins. *Mol. Biol. Cell* **21,** 1922–1936
14. Deplus, R., Delatte, B., Schwinn, M. K., Defrance, M., Méndez, J., Murphy, N., Dawson, M. A., Volkmar, M., Putmans, P., Calonne, E., Shih, A. H., Levine, R. L., Bernard, O., Mercher, T., Solary, E., *et al.* (2013) TET2 and TET3 regulate GlcNAcylation and H3K4 methylation through OGT and SET1/COMPASS. *EMBO J.* **32,** 645–655
15. Love, D. C., Krause, M. W., and Hanover, J. A. (2010) *O*-GlcNAc cycling: emerging roles in development and epigenetics. *Semin. Cell Dev. Biol.* **21,** 646–654
16. Yang, W. H., Park, S. Y., Nam, H. W., Kim do, H., Kang, J. G., Kang, E. S., Kim, Y. S., Lee, H. C., Kim, K. S., and Cho, J. W. (2008) NFκB activation is associated with its *O*-GlcNAcylation state under hyperglycemic conditions. (2008) *Proc. Natl. Acad. Sci. U.S.A.* **105,** 17345–17350
17. Yang, X., Zhang, F., and Kudlow, J. E. (2002) Recruitment of *O*-GlcNAc transferase to promoters by corepressor mSin3A: coupling protein *O*-GlcNAcylation to transcriptional repression. *Cell* **110,** 69–80
18. Kelly, W. G., and Hart, G. W. (1989) Glycosylation of chromosomal proteins: localization of *O*-linked *N*-acetylglucosamine in *Drosophila* chromatin. *Cell* **57,** 243–251
19. Love, D. C., Ghosh, S., Mondoux, M. A., Fukushige, T., Wang, P., Wilson, M. A., Iser, W. B., Wolkow, C. A., Krause, M. W., and Hanover, J. A. (2010) Dynamic *O*-GlcNAc cycling at promoters of *Caenorhabditis elegans* genes regulating longevity, stress, and immunity. *Proc. Natl. Acad. Sci. U.S.A.* **107,** 7413–7418
20. Chen, Q., Chen, Y., Bian, C., Fujiki, R., and Yu, X. (2013) TET2 promotes histone *O*-GlcNAcylation during gene transcription. *Nature* **493,** 561–564
21. Gagnon, J., Daou, S., Zamorano, N., Iannantuono, N. V., Hammond-Martel, I., Mashtalir, N., Bonneil, E., Wurtele, H., Thibault, P., and Affar el, B. (2015) Undetectable histone *O*-GlcNAcylation in mammalian cells. (2015) *Epigenetics* **10,** 677–691
22. Hart, G. W., Housley, M. P., and Slawson, C. (2007) Cycling of *O*-linked β-*N*-acetylglucosamine on nucleocytoplasmic proteins. *Nature* **446,** 1017–1022
23. Jackson, S. P., and Tjian, R. (1988) *O*-Glycosylation of eukaryotic transcription factors: implications for mechanisms of transcriptional regulation. *Cell* **55,** 125–133
24. Cheng, X., and Hart, G. W. (2001) Alternative *O*-glycosylation/*O*-phosphorylation of serine-16 in murine estrogen receptor β: post-translational regulation of turnover and transactivation activity. *J. Biol. Chem.* **276,** 10570–10575
25. Housley, M. P., Udeshi, N. D., Rodgers, J. T., Shabanowitz, J., Puigserver, P., Hunt, D. F., and Hart, G. W. (2009) A PGC-1α-*O*-GlcNAc transferase complex regulates FoxO transcription factor activity in response to glucose. *J. Biol. Chem.* **284,** 5148–5157
26. Jackson, S. P., and Tjian, R. (1989) Purification and analysis of RNA polymerase II transcription factors by using wheat germ agglutinin affinity chromatography. *Proc. Natl. Acad. Sci. U.S.A.* **86,** 1781–1785
27. Capotosti, F., Guernier, S., Lammers, F., Waridel, P., Cai, Y., Jin, J., Conaway, J. W., Conaway, R. C., and Herr, W. (2011) *O*-GlcNAc transferase catalyzes site-specific proteolysis of HCF-1. *Cell* **144,** 376–388
28. Slawson, C., Zachara, N. E., Vosseller, K., Cheung, W. D., Lane, M. D., and Hart, G. W. (2005) Perturbations in *O*-linked β-*N*-acetylglucosamine protein modification cause severe defects in mitotic progression and cytokinesis. *J. Biol. Chem.* **280,** 32944–32956
29. Sakabe, K., Wang, Z., and Hart, G. W. (2010) β-*N*-Acetylglucosamine (*O*-GlcNAc) is part of the histone code. *Proc. Natl. Acad. Sci. U.S.A.* **107,** 19915–19920
30. Zhang, S., Roche, K., Nasheuer, H. P., and Lowndes, N. F. (2011) Modification of histones by sugar β-*N*-acetylglucosamine (GlcNAc) occurs on multiple residues, including histone H3 serine 10, and is cell cycle-regulated. *J. Biol. Chem.* **286,** 37483–37495
31. Worby, C. A., Simonson-Leff, N., and Dixon, J. E. (2001) RNA interference of gene expression (RNAi) in cultured *Drosophila* cells. *Sci. STKE* **2001,** pl1
32. Brown, J. L., Fritsch, C., Mueller, J., and Kassis, J. A. (2003) The *Drosophila* pho-like gene encodes a YY1-related DNA binding protein that is redundant with pleiohomeotic in homeotic gene silencing. *Development* **130,** 285–294
33. Dietzl, G., Chen, D., Schnorrer, F., Su, K. C., Barinova, Y., Fellner, M., Gasser, B., Kinsey, K., Oppel, S., Scheiblauer, S., Couto, A., Marra, V., Keleman, K., and Dickson, B. J. (2007) A genome-wide transgenic RNAi library for conditional gene inactivation in *Drosophila*. *Nature* **448,** 151–156
34. Kaasik, K., Kivimäe, S., Allen, J. J., Chalkley, R. J., Huang, Y., Baer, K., Kissel, H., Burlingame, A. L., Shokat, K. M., Ptáček, L. J., and Fu, Y. H. (2013) Glucose sensor *O*-GlcNAcylation coordinates with phosphorylation to regulate circadian clock. *Cell Metab.* **17,** 291–302
35. Ashburner, M., Golic, K. G., and Hawley, R. S. (2005) *Drosophila: A Laboratory Handbook,* Cold Spring Harbor Laboratory Press, Cold Spring Harbor, NY
36. Xu, T., and Rubin, G. M. (1993) Analysis of genetic mosaics in developing

and adult *Drosophila* tissues. *Development* **117,** 1223–1237
37. Lavrov, S., Déjardin, J., and Cavalli, G. (2004) Combined immunostaining and FISH analysis of polytene chromosomes. *Methods Mol. Biol.* **247,** 289–303
38. Mohan, M., Herz, H. M., Smith, E. R., Zhang, Y., Jackson, J., Washburn, M. P., Florens, L., Eissenberg, J. C., and Shilatifard, A. (2011) The COMPASS family of H3K4 methylases in *Drosophila*. *Mol. Cell. Biol.* **31,** 4310–4318
39. Kim, E. J., Kang, D. O., Love, D. C., and Hanover, J. A. (2006) Enzymatic characterization of *O*-GlcNAcase isoforms using a fluorogenic GlcNAc substrate. *Carbohydr. Res.* **341,** 971–982
40. Hanover, J. A., Krause, M. W., and Love, D. C. (2012) Bittersweet memories: linking metabolism to epigenetics through *O*-GlcNAcylation. *Nat. Rev. Mol. Cell Biol.* **13,** 312–321
41. Steffen, P. A., and Ringrose, L. (2014) What are memories made of? how Polycomb and Trithorax proteins mediate epigenetic memory. *Nat. Rev. Mol. Cell Biol.* **15,** 340–356
42. Huang da, W., Sherman, B. T., and Lempicki, R. A. (2009) Systematic and integrative analysis of large gene lists using DAVID bioinformatics resources. *Nat. Protoc.* **4,** 44–57
43. Bellen, H. J., Levis, R. W., Liao, G., He, Y., Carlson, J. W., Tsang, G., Evans-Holm, M., Hiesinger, P. R., Schulze, K. L., Rubin, G. M., Hoskins, R. A., and Spradling, A. C. (2004) The BDGP gene disruption project: single transposon insertions associated with 40% of *Drosophila* genes. *Genetics* **167,** 761–781
44. Ardehali, M. B., Mei, A., Zobeck, K. L., Caron, M., Lis, J. T., and Kusch, T. (2011) *Drosophila* Set1 is the major histone H3 lysine 4 trimethyltransferase with role in transcription. *EMBO J.* **30,** 2817–2828
45. Kuzin, B., Tillib, S., Sedkov, Y., Mizrokhi, L., and Mazo, A. (1994) The *Drosophila* trithorax gene encodes a chromosomal protein and directly regulates the region-specific homeotic gene fork head. *Genes Dev.* **8,** 2478–2490
46. Xuan, T., Xin, T., He, J., Tan, J., Gao, Y., Feng, S., He, L., Zhao, G., and Li, M. (2013) dBre1/dSet1-dependent pathway for histone H3K4 trimethylation has essential roles in controlling germline stem cell maintenance and germ cell differentiation in the *Drosophila* ovary. *Dev. Biol.* **379,** 167–181
47. McClain, D. A., Lubas, W. A., Cooksey, R. C., Hazel, M., Parker, G. J., Love, D. C., and Hanover, J. A. (2002) Altered glycan-dependent signaling induces insulin resistance and hyperleptinemia. *Proc. Natl. Acad. Sci. U.S.A.* **99,** 10695–10699
48. Vosseller, K., Wells, L., Lane, M. D., and Hart, G. W. (2002) Elevated nucleocytoplasmic glycosylation by *O*-GlcNAc results in insulin resistance associated with defects in Akt activation in 3T3-L1 adipocytes. *Proc. Natl. Acad. Sci. U.S.A.* **99,** 5313–5318
49. Shafi, R., Iyer, S. P., Ellies, L. G., O'Donnell, N., Marek, K. W., Chui, D., Hart, G. W., and Marth, J. D. (2000) The *O*-GlcNAc transferase gene resides on the X chromosome and is essential for embryonic stem cell viability and mouse ontogeny. *Proc. Natl. Acad. Sci. U.S.A.* **97,** 5735–5739
50. Keembiyehetty, C., Love, D. C., Harwood, K. R., Gavrilova, O., Comly, M. E., and Hanover, J. A. (2015) Conditional knock-out reveals a requirement for *O*-linked *N*-acetylglucosaminase (*O*-GlcNAcase) in metabolic homeostasis. *J. Biol. Chem.* **290,** 7097–7113
51. Yang, Y. R., Song, M., Lee, H., Jeon, Y., Choi, E. J., Jang, H. J., Moon, H. Y., Byun, H. Y., Kim, E. K., Kim, D. H., Lee, M. N., Koh, A., Ghim, J., Choi, J. H., Lee-Kwon, W., *et al*. (2012) *O*-GlcNAcase is essential for embryonic development and maintenance of genomic stability. *Aging Cell* **11,** 439–448
52. Rodriguez-Jato, S., Busturia, A., and Herr, W. (2011) *Drosophila melanogaster* dHCF interacts with both PcG and TrxG epigenetic regulators. *PLoS ONE* **6,** e27479
53. Wysocka, J., Myers, M. P., Laherty, C. D., Eisenman, R. N., and Herr, W. (2003) Human Sin3 deacetylase and trithorax-related Set1/Ash2 histone H3-K4 methyltransferase are tethered together selectively by the cell-proliferation factor HCF-1. *Genes Dev.* **17,** 896–911
54. Yan, D., Neumüller, R. A., Buckner, M., Ayers, K., Li, H., Hu, Y., Yang-Zhou, D., Pan, L., Wang, X., Kelley, C., Vinayagam, A., Binari, R., Randklev, S., Perkins, L. A., Xie, T., *et al*. (2014) A regulatory network of *Drosophila* germline stem cell self-renewal. *Dev. Cell* **28,** 459–473
55. Howerton, C. L., Morgan, C. P., Fischer, D. B., and Bale, T. L. (2013) *O*-GlcNAc transferase (OGT) as a placental biomarker of maternal stress and reprogramming of CNS gene transcription in development. *Proc. Natl. Acad. Sci. U.S.A.* **110,** 5169–5174
56. Feller, C., Forné, I., Imhof, A., and Becker, P. B. (2015) Global and specific responses of the histone acetylome to systematic perturbation. *Mol. Cell* **57,** 559–571